Variability of aerosol parameters over Kanpur, northern India

R. P. Singh,[1] Sagnik Dey, S. N. Tripathi, and Vinod Tare
Department of Civil Engineering, Indian Institute of Technology, Kanpur, India

Brent Holben
NASA Goddard Space Flight Center, Greenbelt, Maryland, USA

Received 28 April 2004; revised 2 August 2004; accepted 5 October 2004; published 11 December 2004.

[1] Aerosol optical properties and the spectral behavior of the aerosol optical depth (AOD) over Kanpur, an urban-industrial city in the Ganga basin, have been presented for the first time. Measurements by the ground-based Aerosol Robotic Network (AERONET) during January 2001 to December 2003 show pronounced seasonal influence, with maximum dust loading during the premonsoon season (April–May). The distribution of AOD is found to be large with a mean value of 0.6 at 500 nm wavelength. The frequency distribution of the Ångström parameter α reveals two modes ($\alpha < 1$ dominant dusty condition and $\alpha > 1$ urban aerosols). Diurnal variations of AOD, water vapor content (WVC), and Ångström parameter show strong seasonal influence. Maximum variation of AOD is found during the monsoon season (presence of mixed types of aerosols), maximum variation of WVC is observed during the winter season (frequent changes in humidity and air pressure), and α shows maximum variations during the premonsoon (dust dominating the atmospheric optical conditions) season. The aerosol volume size distributions show two distinct modes, fine (geometric mean radii of 0.17 μm and standard deviation of 0.03) and coarse (geometric mean radii of 3.37 μm and standard deviation of 0.1), but during May–August (period of dust loading), a third mode (around 1–2 μm) appears because of hygroscopic growth of finer aerosols. The single-scattering albedo (SSA) is found to increase with wavelength in the presence of dust and shows a reverse trend in dust-free conditions. Refractive indices show the presence of dust as the main component during the premonsoon season and dominance of anthropogenic urban-industrial aerosols during the winter season, when the optical state of the atmosphere is more absorbing. The aerosol parameters show distinct interannual variations, with increasing aerosol burden over the region. Aerosol loading over Kanpur is found to be controlled by the regional climatology. *INDEX TERMS:* 0305 Atmospheric Composition and Structure: Aerosols and particles (0345, 4801); 0345 Atmospheric Composition and Structure: Pollution—urban and regional (0305); 3309 Meteorology and Atmospheric Dynamics: Climatology (1620); 3359 Meteorology and Atmospheric Dynamics: Radiative processes; 3360 Meteorology and Atmospheric Dynamics: Remote sensing; *KEYWORDS:* aerosol, remote sensing, Ganga basin

Citation: Singh, R. P., S. Dey, S. N. Tripathi, V. Tare, and B. Holben (2004), Variability of aerosol parameters over Kanpur, northern India, *J. Geophys. Res.*, *109*, D23206, doi:10.1029/2004JD004966.

1. Introduction

[2] Kanpur (longitude 80°20′E and latitude 26°26′N) is one of the industrial cities, with 3.2 million population, situated in the southern flank of the central part of the Ganga basin. Ganga basin is one of the largest drainage basins in the world and is bordered by the Himalayas to the north and Vindhyan-Satpura ranges to the south. The Ganga basin is traversed by the two main rivers Ganga and Yamuna and their tributaries. Because of the growing urbanization and economic growth, the rural population is migrating to urban areas particularly in India and in general in Asia. *Guttikunda et al.* [2003] studied the contribution of megacities to sulfur emission and pollution in Asia over a 25-year period (1975–2000) using a multilayer Lagrangian puff transport model and have found that Asian megacities cover <2% of the land area but emit ~16% of the total anthropogenic sulfur emission of Asia. They have shown that urban sulfur emissions contribute over 30% to the regional pollution levels in large parts of Asia. With the growing population, the land use, land cover, and density of industries have increased many fold in the last 40 years, and as a result the pollution level has also increased. The increase in the pollution level and high aerosol loading over

[1]Now at School of Computational Sciences, George Mason University, Fairfax, Virginia, USA.

0148-0227/04/2004JD004966$09.00

the Ganga basin has been found by *Goloub et al.* [2001] using ADEOS POLDER data. The increase of pollution has a direct impact on climatic conditions, especially the increase of haze, fog, and cloudy conditions, which decrease the visibility especially during the winter season. The major pollutant in the Ganga basin is sulfate aerosols due to growing anthropogenic activities [*Sharma et al.*, 2003]. In the northern India, suspended particulate matter concentration is higher during the summer season compared to that during the winter season, reducing the neutralization capacity of the atmosphere [*Sharma et al.*, 1994]. Measurements by Central Pollution Control Board (CPCB) have also shown very high annual average concentrations (>210 $\mu g/m^3$, in the critical range compared to the air quality standard in India) of particulate matter of diameter less than 10 μm (PM_{10}) in the atmosphere of the major cities of the Ganga basin (CPCB, 2002, http://www.cpcb.nic.in). In addition to the urban-industrial pollution, desert dust is another major source of the aerosols over the Ganga basin [*Dey et al.*, 2004; *El-Askary et al.*, 2004]. Considering the increasing aerosol loading over Asia, several ground-based aerosol monitoring stations have been established in east and Southeast Asia, and the long-term measurements of aerosol climatology have been reported by *Kim et al.* [2004] for east Asia.

[3] Information about the emission of pollutants helps in understanding the anthropogenic perturbations in aerosol climatology. *Reddy and Venkataraman* [2002] have constructed a spatially resolved emission inventory for India to serve as an input to aerosol-climate studies. Uncertainties in quantifying the radiative forcing of the climate accurately [*Charlson et al.*, 1992; *Tegen et al.*, 1996; *Hansen et al.*, 1997; *Satheesh and Ramanathan*, 2000; Intergovernmental Panel on Climate Change, 2001, http://www.ipcc.ch] are due to incomplete knowledge of the macrophysical (sources, sinks, and loading) and microphysical (composition, size distribution, diurnal variation, optical properties, and lifetime) [*Dubovik et al.*, 2000, 2002] properties of aerosols. In India, routine measurements of aerosols started in the late 1980s in Trivandram (southwestern coastal city of India) and in a few cities in the southern part of India [*Sikka*, 2002]. A network of seven stations (each representing a particular environment) has been established in India (shown as solid circles in Figure 1) under the Indian Space Research Organization Geosphere Biosphere Program (ISRO-GBP) for monitoring of aerosols, where a multiwavelength solar radiometer is deployed [*Krishna Moorthy et al.*, 1999]. Considering the variability of the meteorological parameters over the Indian subcontinent, a few aerosol monitoring stations are not enough to understand the atmospheric dynamics and climatology. Studies during the Indian Ocean Experiment (INDOEX) have shown that ~70% of aerosol load over the oceanic regions surrounding India during winter is of anthropogenic origin [*Ramanathan et al.*, 2001]. *Eck et al.* [2001] have studied the effect of the monsoon on aerosol optical properties over the Indian Ocean using ground-based Sun and sky radiometer.

[4] Long-term monitoring has been carried out under the Aerosol Robotic Network (AERONET) program to characterize different types of aerosols [*Smirnov et al.*, 1996, 2002a, 2002b; *Eck et al.*, 1999, 2003a; *O'Neill et al.*, 2000; *Dubovik et al.*, 2002] in various key locations of the world, and also several campaign mode studies have been conducted to understand the spatiotemporal distribution of the aerosol optical properties [*Smirnov et al.*, 1998, 2000a; *Remer et al.*, 1999; *O'Neill et al.*, 2002; *Eck et al.*, 2003b]. In India, efforts have been made to study aerosol behavior in some urban cities (mainly coastal cities with influence of marine aerosols) [*Niranjan et al.*, 1997; *Parameswaran*, 1998; *Babu and Moorthy*, 2001; *Venkataraman et al.*, 2002]; no detailed study with continuous measurements has been carried out in the Ganga basin. In the present study, we analyze the aerosol parameters over Kanpur on the basis of routine measurements using an automatic Sun and sky radiometer during 2001–2003. Our analysis shows strong spectral, seasonal, and interannual variability of the optical properties of the aerosols over Kanpur.

2. Site Characterization, Instrumentation, and Data Analyses

[5] For continuous monitoring of aerosols over the Ganga basin, a CIMEL radiometer was deployed on the campus of Indian Institute of Technology (IIT), Kanpur (80°22′E, 26°26′N, and 142 m altitude from mean sea level), as a part of the AERONET program in January 2001. The IIT Kanpur campus is ~17 km away from the center of Kanpur (shown in Figure 1). Kanpur is a representative site of the Ganga basin in terms of the weather conditions and atmospheric seasonal variability. The Ganga basin experiences four dominant seasons each year: winter (December-February), premonsoon (March–May), monsoon (June–August), and postmonsoon (September–November). During the premonsoon and monsoon seasons, air mass carries dry dust particles from the western Thar Desert to the region, and during the postmonsoon and winter seasons, air mass flows from the north and northwest, bringing finer continental aerosols (Figure 1). The premonsoon season is characterized by frequent dust storms and dry weather (relative humidity varies within the range of 25–50%). Monsoon wind arrives in the region from the eastern part of the Ganga basin during late June to early July carrying moisture, and as a result the relative humidity increases drastically up to 60–90% range. During the winter season, whole parts of northern India suffer from western disturbances (a series of alternate low- and high-pressure areas), which move from west to east, leading to intense fog and haze in the region [*Pasricha et al.*, 2003].

[6] The Sun/sky radiometer is located on top of a roof with no obstructions to the Sun above 10^0 elevation. The CIMEL radiometer takes measurements of the direct Sun and diffuse sky radiances within the spectral range 340–1020 nm [*Holben et al.*, 1998]. The direct Sun measurements are made at eight spectral channels (340, 380, 440, 500, 670, 870, 940, and 1020 nm) with triplet observations per wavelength and sky measurements at four spectral channels (440, 670, 870, and 1020 nm) to deduce aerosol optical properties. The 940-nm channel is used to estimate the water vapor content (WVC), and the remaining seven channels are used to retrieve aerosol optical depth (AOD). The uncertainty in calculation of AOD under cloud-free conditions is less than ±0.01 for $\lambda > 440$ nm and less than ±0.02 for shorter wavelengths, is ±10% for retrieval of

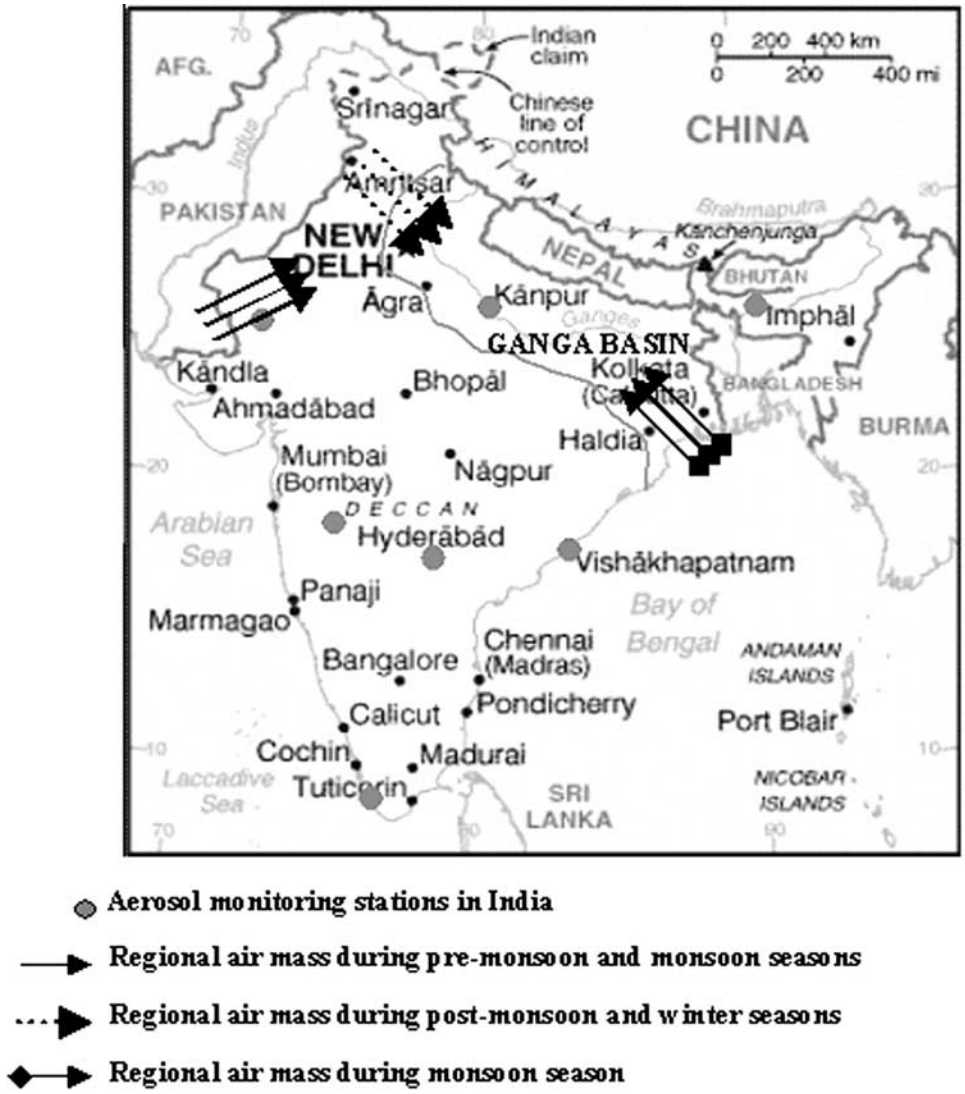

Figure 1. Study area showing the regional air mass during different seasons.

CWV, and is less than ±5% for the sky radiance measurements [*Dubovik et al.*, 2000].

[7] The Sun and sky radiance measurements yield two types of errors, systematic and random [*Dubovik et al.*, 2000], depending on the nature of the aerosols. Even in the so-called error-free conditions (neither systematic nor random errors are specifically introduced in the forward simulations or in the inversion algorithms), some minor errors exist, which can be considered as relative errors with standard deviation <1% for all three major aerosol types, water-soluble, dust, and biomass-burning aerosol [*Dubovik et al.*, 2000]. The errors are not significant for the particles of radius R in the range 0.1–7 μm. The tendency for increasing errors in retrieval of optical properties with the decrease in optical depth is higher in the case of refractive index and single-scattering albedo than in the case of volume size distribution [*Dubovik et al.*, 2000]. The aerosol optical depth data are provided in three categories: cloud-contaminated (level 1.0), cloud-screened (level 1.5), following the methodology described by *Smirnov et al.* [2000b], and quality-assured (level 2.0), which has been used for the present study. The optical properties during the monsoon season in 2003 are missing because of technical problems.

3. Results and Discussion

3.1. Seasonal Variability

[8] Aerosol parameters are characterized by AOD τ_a and Ångström parameter α. Parameter α is computed from a linear fit of log (AOD) versus log (wavelength) according to the classical equation of *Ångström* [1964]

$$\tau_a = \beta\lambda^{-\alpha},$$

where β is the turbidity coefficient and λ is the wavelength. The Ångström fit does not represent all optical depth spectra; it can be considered as a first-order indicator of the average spectral behavior [*Kaufman*, 1993; *Eck et al.*, 1999;

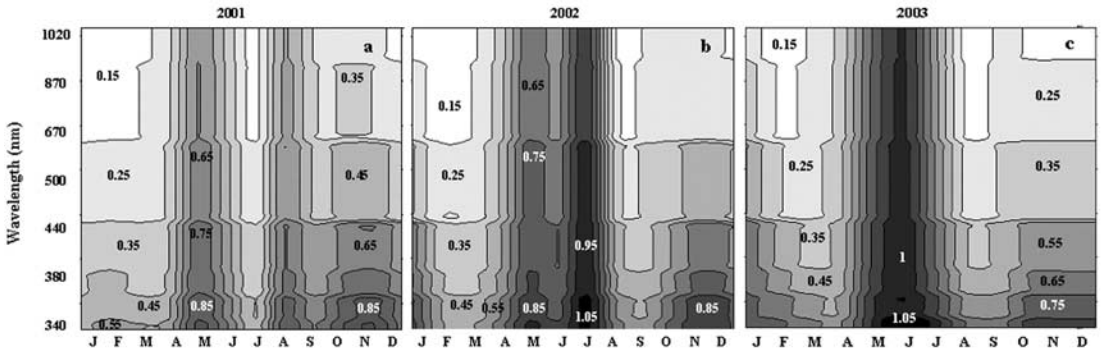

Figure 2. Spectral variations of AOD in (a) 2001, (b) 2002, and (c) 2003.

Cachorro et al., 2001; *O'Neill et al.*, 2001]. Parameter τ_a gives an indication of the amount of aerosol present in the atmosphere, and α gives an indication of the aerosol size distribution.

[9] Figures 2a–2c show the strong seasonal variability of AOD over Kanpur in the wavelength range 340–1020 nm for the years 2001, 2002, and 2003, respectively. AOD spectra reveal interannual variability over Kanpur. The spectral variation of AOD shows two peaks during the months of April–May and July–August in 2001, but these peaks are found to be closer in 2002, with two major peaks in May and July that merge into a single peak in June 2003. The gradual change in spectral and seasonal variability peaks of AOD in 3 years may be due to natural changes or fluctuations in transport and meteorology and will be clearer if studied for longer time period. It is also noted that AOD values are almost similar during the postmonsoon and winter seasons. AOD varies from 0.25 to 0.85 in the year 2001; the highest value is observed in the month of May. In the years 2002 and 2003, AOD increases up to 1.05 in the month of July. AOD has been found to be lowest in the month of January ($\sim$0.25). Increase in AOD is very sharp from the month of April to September, whereas from October to April the changes are not rapid. The rapid increase in AOD during April–May is attributed to the premonsoon dust loading, which reduces the spectral variability. Maximum spectral variation of AOD has been found during the postmonsoon and winter seasons in all 3 years.

[10] Figures 3a–3c show the monthly averaged AOD, WVC, and α for the years 2001–2003 over Kanpur. A total of 852 daily average data of AOD, WVC, and α have been considered (Figures 3d–3f). The mean and standard deviations of AOD are found to be 0.57 and 0.27 during winter, 0.54 and 0.26 during the premonsoon, 0.66 and 0.36 during the monsoon, and 0.63 and 0.23 during the postmonsoon, respectively, which indicates higher variability during the monsoon season. The anual average of AOD at 500 nm, $\tau_{a,500}$, has been found to increase every year ($\tau_{a,500}$ = 0.62 in 2001, 0.644 in 2002, and 0.696 in 2003), indicating an increase in the aerosol burden over the region. WVC varies in the range 0.8–6.8 cm, with the maxima peak during July–August (monsoon time). The mean and standard deviations of WVC are found to be 1.5 and 0.6 (winter), 2.35 and 1.01 (premonsoon), 5.85 and 1.08 (monsoon), and 3.04 and 1.4 (postmonsoon), respectively. Compared to $\tau_{a,500}$, the annual average of WVC over the region shows no increasing trend (3.405 cm in 2001, 3.028 cm in 2002, and 3.357 cm in 2003). WVC during the postmonsoon season is similar to the annual average and shows maximum variability. Parameter α varies in the range 0.1–1.7. The mean and standard deviation of α are 1.26 and 0.25 during winter, 0.6 and 0.31 during the premonsoon, 0.66 and 0.45 during the monsoon, and 1.12 and 0.28 during the postmonsoon time, respectively. The notable decrease in α during April–June (Figure 3c) is associated with the dust loading. The coarse dust particles lead to a higher increase in AOD at higher λ than the increase in AOD at lower λ. This ultimately decreases the spectral dependence of AOD. The annual pattern with maximum aerosol loading during the period May–August (AOD sometime increases above 1.25) and minimum aerosol loading during the period December–February (AOD < 0.25) are evident (Figure 2). Higher fluctuations of AOD are observed in the year 2002 compared to the year 2001 during the premonsoon to monsoon periods because of more frequent dust storms in the year 2002. During the winter season (December–February), the daily averaged WVC shows higher variations compared to other seasons. However, AOD and α show maximum variability during the monsoon season, when air masses from different parts of the basin carry different types of aerosols.

[11] PM_{10} concentrations over Kanpur and several cities are continuously measured by the Central Pollution Control Board (CPCB), India. Figure 4 shows an *X-Y* scatterplot between PM_{10} concentration and $\tau_{a,500}$ over Kanpur during May 2001 to July 2002. Although $\tau_{a,500}$ shows a general increasing trend with higher PM_{10} concentration, the poor correlation (R^2 = 0.06) shows that no direct relationship exists. *Chu et al.* [2003] have found good correlation ($R^2 \sim$ 0.82) between PM_{10} and $\tau_{a,500}$ in northern Italy, arising because of fixed pollution sources and stable air masses. The topography in this region aids in accumulation of the local pollutants under stable conditions without mixing with other aerosol types. The topography of Kanpur is not favorable to allow the pollutants to accumulate under stagnant conditions. Moreover, mixing with other types of aerosols and hygroscopicity are likely to be the reasons for such a poor correlation over Kanpur.

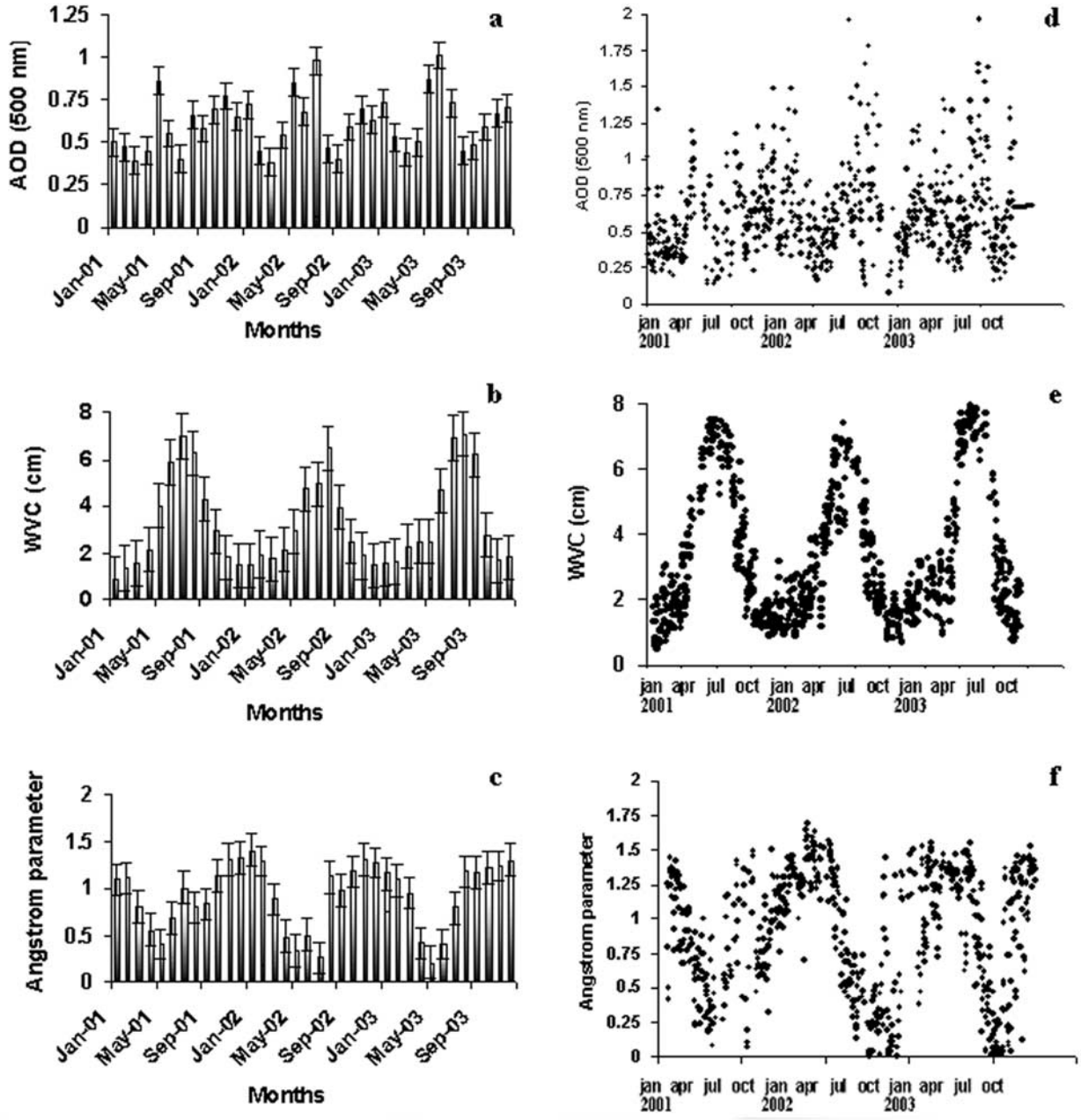

Figure 3. Monthly average and daily average of AOD (Figures 3a and 3d), WVC (Figures 3b and 3e), and Ångström parameter (Figures 3c and 3f) over Kanpur for 3 years. Bars indicate ±1 standard deviation.

[12] Figure 5 shows the frequency distribution of daily averaged AOD, WVC, and α over Kanpur. The distribution of α is relatively broad with two modes (though not very distinct), dusty ($\alpha < 1$) and dust-free ($\alpha > 1$); the dust-free class (49.44%) and the dusty class (50.56%) are found to exist in equal proportion. During the premonsoon season the α peak of the dusty class is found around 0.7 (Figure 6), which is similar to the results found by *Smirnov et al.* [2002a] over the Persian Gulf. The wider frequency distribution of α indicates the abundance of mixed types of aerosols. The AOD distribution is unimodal with a modal value of 0.55. The distribution of WVC is also unimodal (modal value is 2 cm), but the distribution is wide at the higher values, showing a strong seasonal effect. The seasonal frequency distribution of AOD (Figure 6) shows a bimodal nature during June–August (monsoon season), with two distinct modes (modal values of 0.25 and 0.65–0.75). In other seasons, the modal values of AOD distribution lie close to yearly averaged modal values (Figure 6). The seasonal frequency distribution of WVC (Figure 6) reveals the seasonal effect with the modal value increasing from 1.5 cm (during winter) to 6.5–7 cm (during the

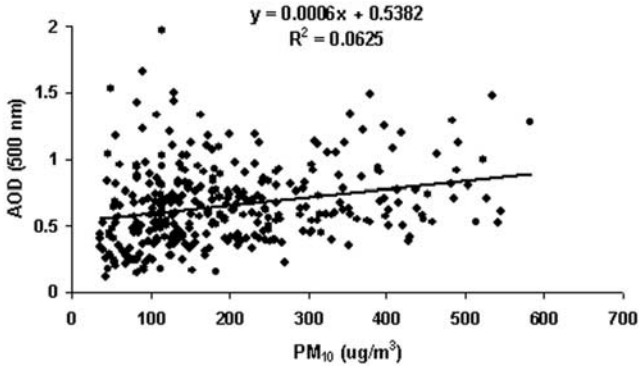

Figure 4. Scatterplot of PM_{10} concentration and AOD (500 nm) over Kanpur.

monsoon). The distribution of WVC is found to be wide during the postmonsoon season, though the modal value is close to the yearly averaged value. The frequency distribution of α shows the dominance of urban aerosols transported by northerly to northwesterly winds during the postmonsoon to winter seasons (α peaks show in the range 1.3–1.5). Dust is brought by the southwesterly wind during the premonsoon season, which is evident in the α frequency distribution (the α peak shifts to 0.7) and remains until monsoon (bimodal distribution), when the atmosphere is characterized by the presence of both dust (modal value is 0.3) and urban aerosols (modal value is 1.3).

3.2. Diurnal Variability of Optical Parameters and Water Vapor Content

[13] Diurnal variability of aerosol optical parameters and WVC has great importance in atmospheric correction and validation of remote-sensing data and is also useful in the calculation of radiative forcing and studying the interaction of aerosols with clouds and humidity [*Smirnov et al.*, 2002c]. The diurnal variability (averaged for each hour from 0700 to 1800 local time (LT), local noon at 1200 LT) of AOD, WVC, and α shows a strong seasonal effect. All individual observations for a day are expressed as a percentage departure from the daily mean (Figure 7) and the hourly averages (Figure 8).

[14] AOD shows maximum departure from the daily mean in the early morning and the late afternoon, whereas during the monsoon (Figure 7c), the maximum departure from the daily mean is observed at noontime (25–30%). The hourly average of AOD also shows drastic increase in AOD (~0.15) during noontime in this period. Diurnal variability of AOD is found to be less during the premonsoon and postmonsoon seasons. The AOD is found to increase at noon and decrease in the afternoon (Figure 8) during all seasons, which may be attributed to the diurnal cycle of local pollutants arising because of anthropogenic activities. The local cycle is more pronounced during the postmonsoon and winter seasons, when the anthropogenic sources mainly contribute to the observed optical depth.

[15] During the premonsoon, monsoon, and postmonsoon seasons, diurnal variations of WVC are found to be low, whereas during the winter season, maximum diurnal variation of WVC is found. During the postmonsoon season the variation (from the daily mean) is observed during the early morning and late afternoon. During the winter, Kanpur and the surrounding region are characterized by frequent change in the atmospheric pressure within a day [*Pasricha et al.*, 2003]. The low-pressure conditions lead to enhanced WVC in the atmospheric boundary layer followed by a high-pressure situation, which results in clear-sky conditions and temperature inversion, leading to high diurnal variation. The natures of the diurnal variations of AOD and WVC are similar only during the premonsoon season.

[16] The diurnal variations of α are most pronounced in the premonsoon season (Figure 8b), which is characterized by maximum dust loading (α is smaller compared to the other seasons). In this season the diurnal variation of α shows a reverse trend of AOD. This pattern is found to continue during the monsoon (Figure 8c), but the variation

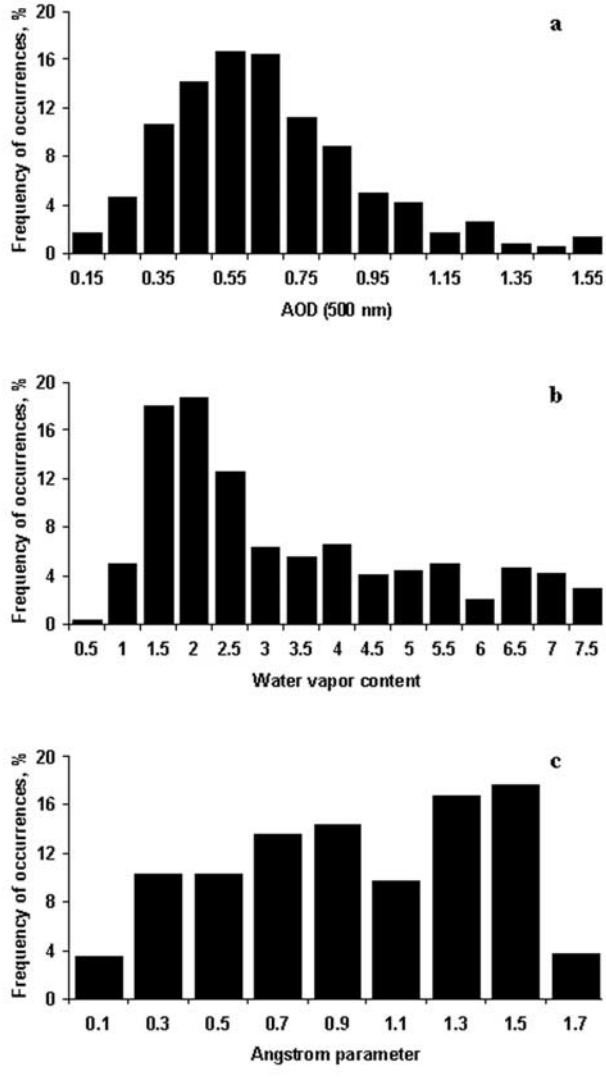

Figure 5. Frequency distribution of the (a) AOD, (b) WVC, and (c) Ångström parameter for the daily averaged data.

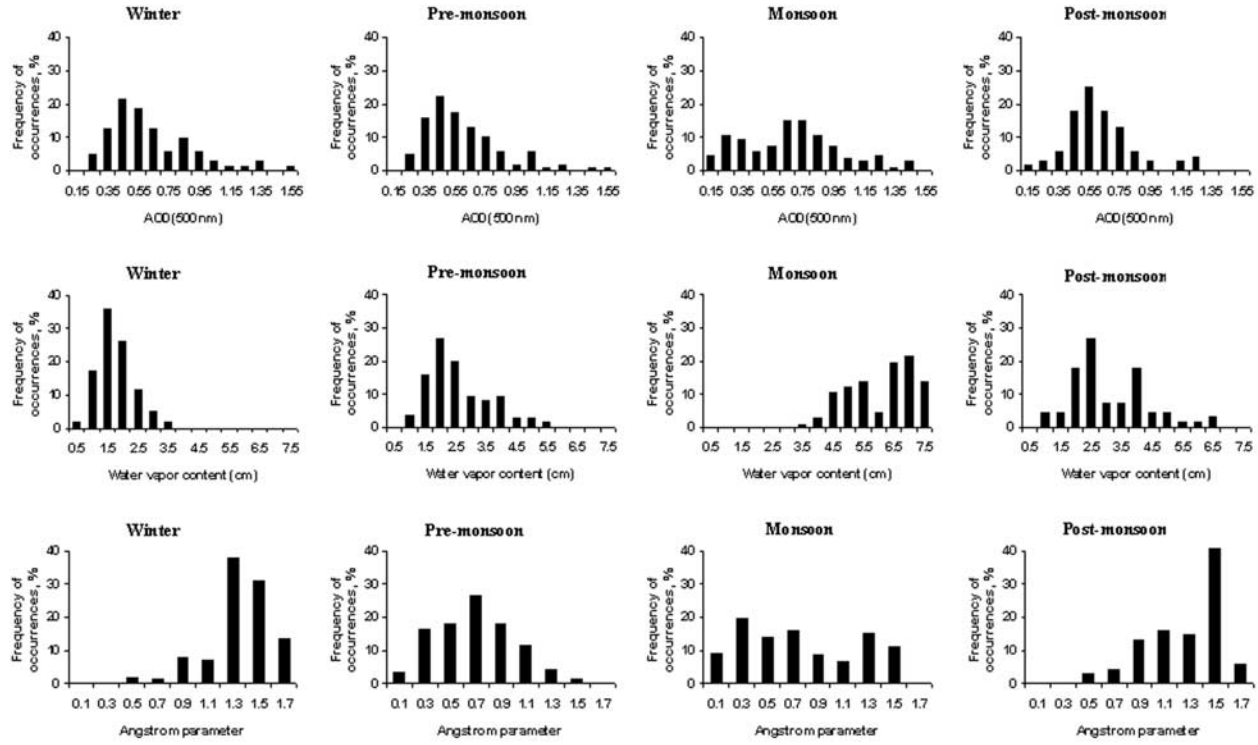

Figure 6. Seasonal frequency of occurrences of AOD, WVC (cm), and Ångström parameter. The sum of frequencies is equal to 100% for each season.

in α is less compared to the variation in premonsoon period. In the postmonsoon and winter seasons (September–February), α shows high variation in the early morning and late afternoon. The hourly average of α increases at midday as a result of maximum local pollutants and the anthropogenic activities during the postmonsoon and winter seasons due to weather conditions, especially low wind velocity (<1.02 m/s).

3.3. Aerosol Volume Size Distributions

[17] The aerosol volume size distribution ($dV/d\ \ln\ R$) has been retrieved from the spectral Sun and sky radiance data using the *Dubovik and King* [2000] approach with the initial guess $dV/d\ \ln\ R = 0.0001$, $n(\lambda_i) = 1.5$, $k(\lambda_i) = 0.005$, where $dV/d\ \ln\ R$ denotes volume size distribution and $n(\lambda_i)$ and $k(\lambda_i)$ are the real and imaginary parts of the refractive index at wavelength λ_i, respectively. Figures 9a, 9b, and 9c show the seasonal aerosol volume size distribution over Kanpur for 2001, 2002, and 2003, respectively. The size distribution reveals two distinct modes: fine (particle size < 0.6 μm) and coarse (particle size > 0.6 μm). The bimodal structure of volume size distribution may be due to various reasons, such as mixing of two air masses with different aerosol populations [*Hoppel et al.*, 1985], homogeneous heteromolecular nucleation of new fine particles in the air, or heterogeneous nucleation and growth of larger particles by condensation of gas-phase reaction products.

[18] Table 1 shows the parameters of the bimodal log-normal volume size distribution; for each mode, the log-normal distribution [*Seinfeld and Pandis*, 1997] is defined as

$$dV/d\ \ln\ R = \left(V/\sigma(2\Pi)^{1/2}\right)\ \exp\left[-0.5\left(\ln\ (R/R_v)^2/\sigma^2\right)\right],$$

where $dV/d\ \ln\ R$ is the volume size distribution, V is the columnar volume of particles per unit cross section of atmospheric column, R is the particle radius, R_v is the volume geometric mean radius, and σ is the geometric standard deviation. The volume geometric mean radius is found to be higher for the fine mode during the postmonsoon to winter seasons (0.129 μm < R_v < 0.148 μm) compared to that during the premonsoon to monsoon seasons (0.065 μm < R_v < 0.17 μm), but it is similar during all seasons for the coarse mode (2.24 μm < R_v < 3.85 μm). The volume concentrations of aerosol particles in two modes (fine and coarse) are found to be similar during the postmonsoon and winter seasons, which is very unusual in an urban site. However, *Dubovik et al.* [2002] have recently found that the urban sites are dominated by fine mode aerosols ($\alpha > 1.7$), whereas over Kanpur the frequency distribution of α (Figure 5c) shows less than 4% values for $\alpha > 1.7$. Even during the postmonsoon and winter seasons, in the absence of prominent dust loading, the frequency of α values greater than 1.7 is ~10%. During the premonsoon and monsoon seasons (April–August) the volume concentration is found to be doubled compared to that during the postmonsoon and winter seasons (Table 1). This type of volume size distribution has been observed by

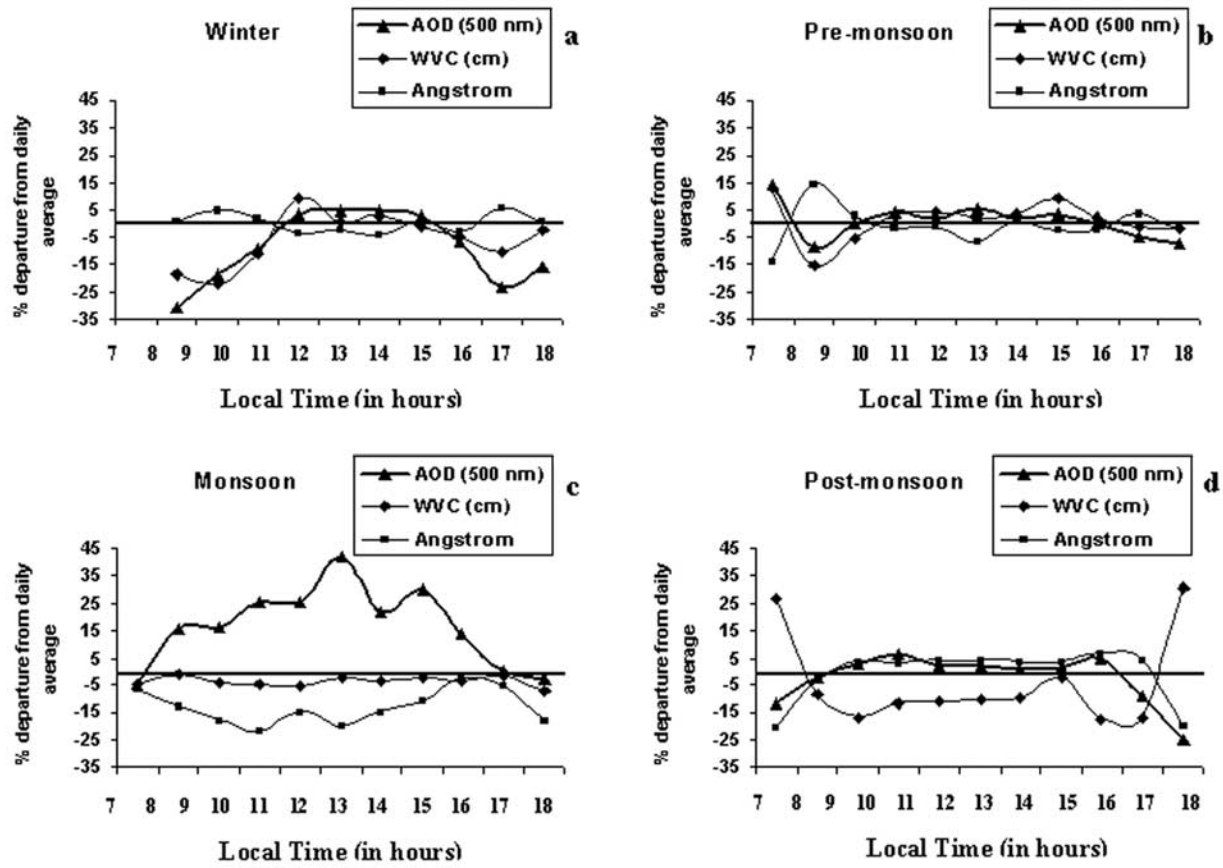

Figure 7. Diurnal variability of AOD, WVC, and Ångström parameter during (a) winter, (b) premonsoon, (c) monsoon, and (d) postmonsoon seasons computed hourly as percentage departure from daily average.

Dubovik et al. [2002] for desert dust aerosols. A higher volume concentration (1.5 times higher) at coarse mode in 2002 than in 2001 and 2003 suggests higher dust loading during that year, which is also evident in AOD spectra and α (Figure 2). The effect of the dust events on the aerosol optical properties in this region has been recently studied by *Dey et al.* [2004], and they have found that aerosol volume concentration at coarse mode increases 3 times after the dust events, without any significant change in volume concentration of fine mode aerosols. Another mode in the size range 1–2 μm has been observed during the premonsoon to monsoon seasons (Figure 9). The finer urban aerosols grow hygroscopically in the presence of abundant atmospheric water vapor [*Parameswaran and Vijayakumar*, 1994] during the premonsoon and monsoon seasons, resulting in the generation of the third mode in the volume size distribution. The fine mode is found to shift toward the coarser mode during the postmonsoon and winter seasons (from $R = 0.1$ to $R = 0.4$ μm), whereas no shift has been observed for the coarse mode aerosols.

[19] The aerosol volume concentration shows higher values in the year 2002 compared to those in the years 2001 and 2003 because of the late arrival of the monsoon in the region, which is also evident from WVC variations (Figure 3b): maximum WVC during August in 2002 compared to maximum WVC during July 2001 and 2003. In 2002, precipitation only occurred on 3 days during June and July, suggesting late arrival of the monsoon wind, whereas in 2001 and 2003, monsoon precipitation started from the end of June. Because of the late arrival of the monsoon, dust particles dominated for a longer period of time because of dominance of the southwesterly wind. However, no interannual variability has been found in the size distribution during the postmonsoon and winter seasons.

3.4. Spectral Dependence of Single-Scattering Albedo (SSA)

[20] Optical properties of urban aerosols depend on the complex combination of natural and anthropogenic factors influencing aerosol formation and evolution. SSA has been computed from the scattering optical thickness approximated from the nonnormalized aerosol-scattering phase function using diffuse radiance measured at different angles [*Dubovik et al.*, 1998]. The spectral variation of SSA is shown in Figures 10a–10c for the years 2001, 2002, and 2003, respectively. SSA (at all wavelengths) has been found to be lower (<0.85) during the winter season compared to that in the other seasons. An increase in SSA values in conjunction with lower α during the premonsoon to monsoon periods in the year 2002 compared to those in the year 2001 indicates higher relative concentration of scattering dust particles to absorbing particles in the atmosphere. The SSA variations in the year 2003 are found to be similar to those of the year 2002 in general (Figure 10), but because of

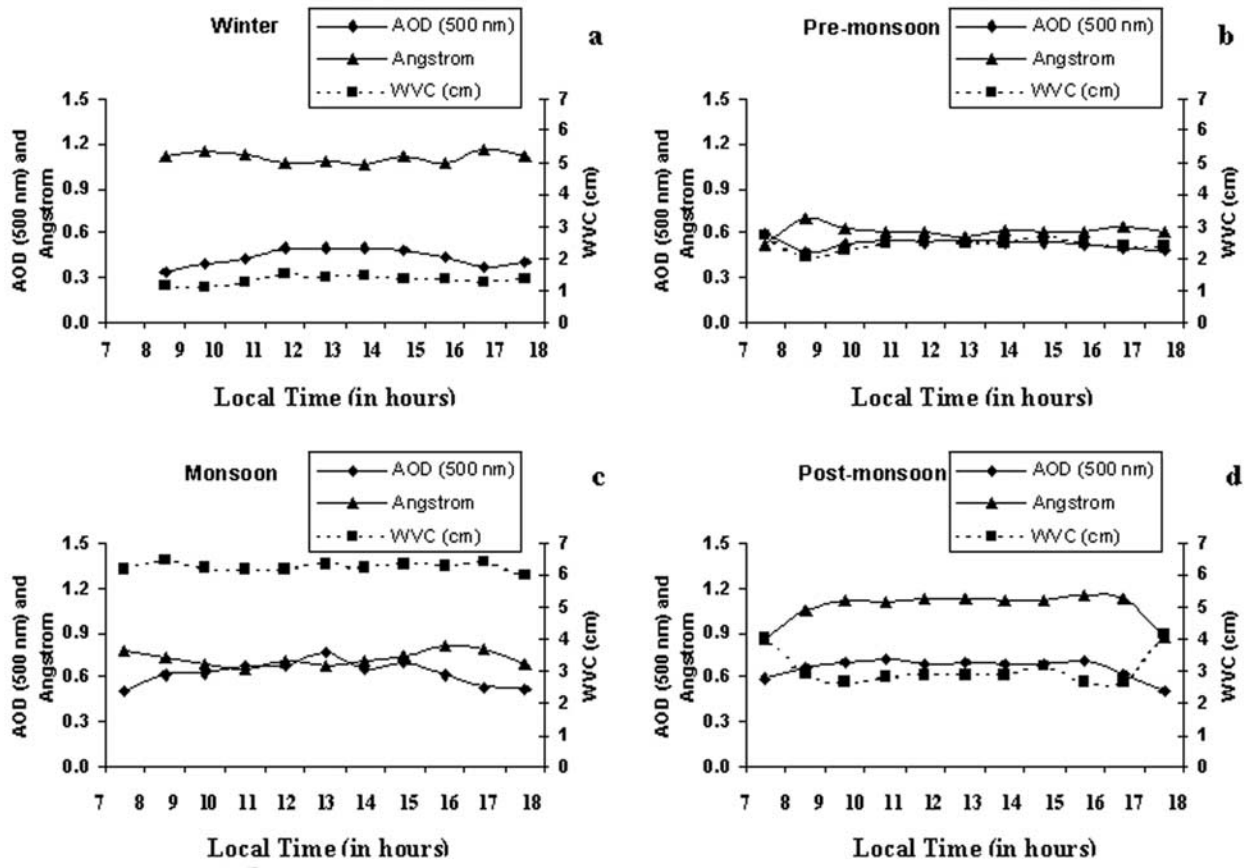

Figure 8. Hourly averages of AOD, WVC, and Ångström parameter during (a) winter, (b) premonsoon, (c) monsoon, and (d) postmonsoon seasons.

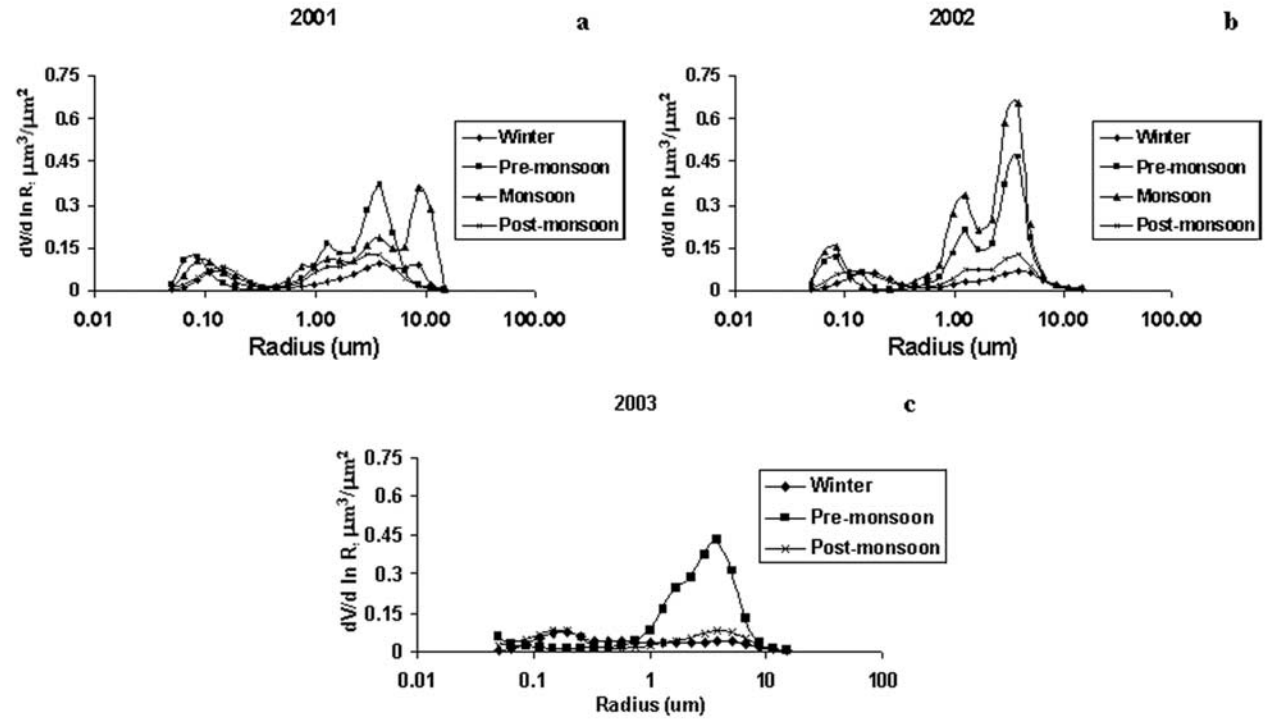

Figure 9. Seasonal aerosol volume size distribution over Kanpur in (a) 2001, (b) 2002, and (c) 2003.

Table 1. Parameters of Aerosol Volume Size Distribution[a]

	Fine Mode			Coarse Mode		
	V	R_v, μm	σ	V	R_v, μm	σ
January	0.024	0.148	0.02	0.033	3.85	0.027
February	0.016	0.148	0.019	0.029	2.939	0.023
March	0.016	0.113	0.015	0.042	2.566	0.049
April	0.019	0.065	0.043	0.059	2.24	0.112
May	0.026	0.17	0.062	0.109	2.566	0.214
June	0.028	0.098	0.039	0.074	2.24	0.112
July	0.031	0.098	0.029	0.109	2.939	0.12
August	0.038	0.098	0.049	0.19	3.85	0.221
September	0.025	0.129	0.026	0.039	2.24	0.055
October	0.026	0.148	0.027	0.038	2.566	0.038
November	0.028	0.148	0.024	0.035	2.939	0.03
December	0.025	0.169	0.023	0.027	2.939	0.023

[a]V is the volume concentration ($\mu m^3\ \mu m^{-2}$), R_v (μm) is the volume geometric mean radius, and σ is the geometric standard deviation.

the absence of monsoon season data (due to technical problems in AERONET operation), no definite conclusions are drawn.

[21] The SSA of the aerosols is found to be strongly wavelength dependent during the winter season, when SSA decreases with increase in wavelength. Absorbing urban aerosols are dominant during the winter season over Kanpur, which shows lower SSA at longer wavelength, as the interaction of these aerosols with the incoming solar radiation is minimum at longer wavelength. During the postmonsoon season, SSA is almost independent of wavelength, whereas during the premonsoon and monsoon seasons, SSA increases with wavelength (Figures 10a, 10b, and 10c), which is attributed to the dominance of coarse particles (mostly dust) [*Ackerman and Toon*, 1981]. Similar spectral variations of SSA have been found by *Smirnov et al.* [2002a] in the Persian Gulf, which indicate that the spectral behavior of SSA depends on the nature of the aerosol particles. In the premonsoon and monsoon (characterized by dust loading), SSA is found to be higher (>0.9), more scattering, compared to the postmonsoon and winter seasons, and characterized by a dominance of finer absorbing urban aerosols. At lower wavelengths the difference in SSA between dusty and finer aerosols is found to be small (0.01 at 440 nm) compared to the difference at longer wavelengths (0.055 at 1020 nm) (Figures 10a, 10b, and 10c). The low SSA at lower wavelengths during the winter season is due to the presence of absorbing aerosols [*Dubovik et al.*, 2002]. The water-soluble aerosols present during the premonsoon and monsoon seasons grow hygroscopically in the presence of water vapor (also evident in the volume size distribution curves in Figure 9) and contribute to higher SSA values at higher wavelengths.

[22] SSA values over Kanpur show significant interannual variation with higher SSA values (>0.93) during the premonsoon and monsoon seasons in the year 2002. This is due to higher loading of water-soluble aerosols from anthropogenic sources and dust (scattering in nature) during 2002 compared to 2001 and 2003. This is also reflected in the AOD and the size distribution data (Figures 2 and 9). The spectral dependency of SSA during the winter season is less during 2002, which indicates a lower concentration of absorbing aerosols in the atmosphere. Spectral variation of SSA during the postmonsoon season in the year 2003 has

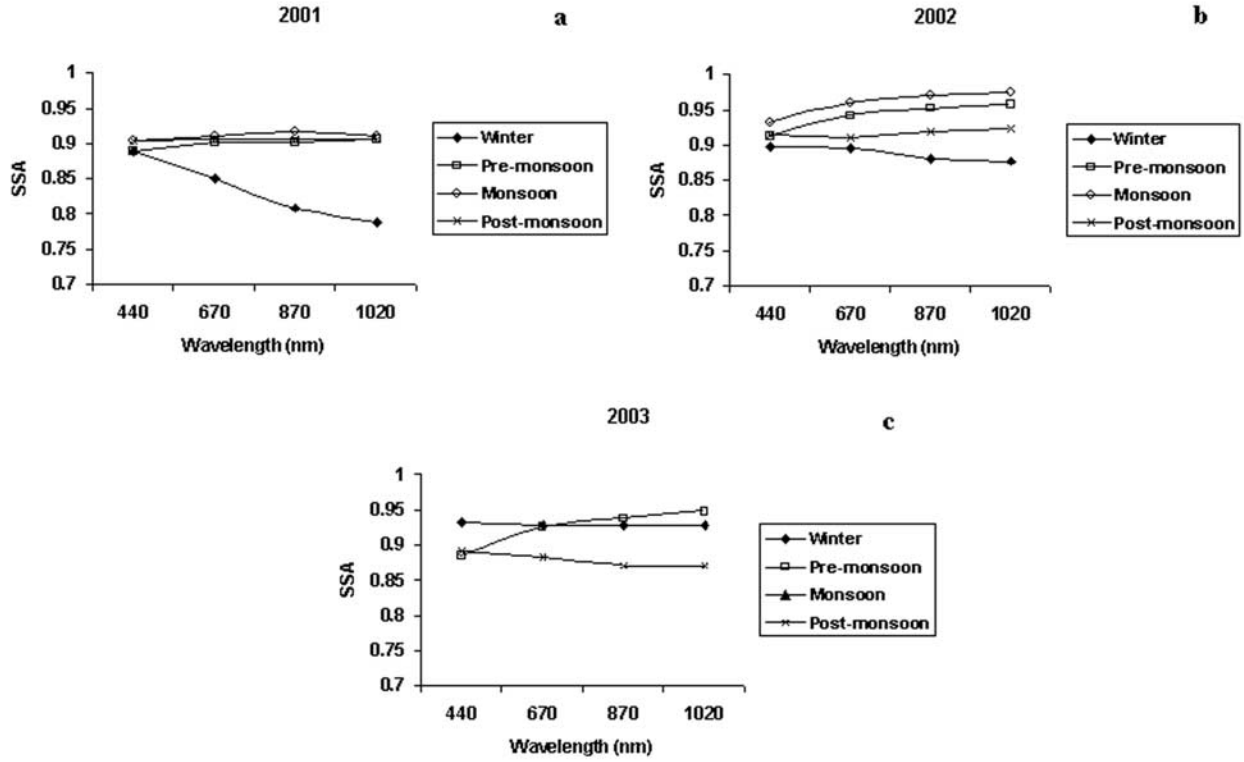

Figure 10. Seasonal variations in SSA for (a) 2001, (b) 2002, and (c) 2003.

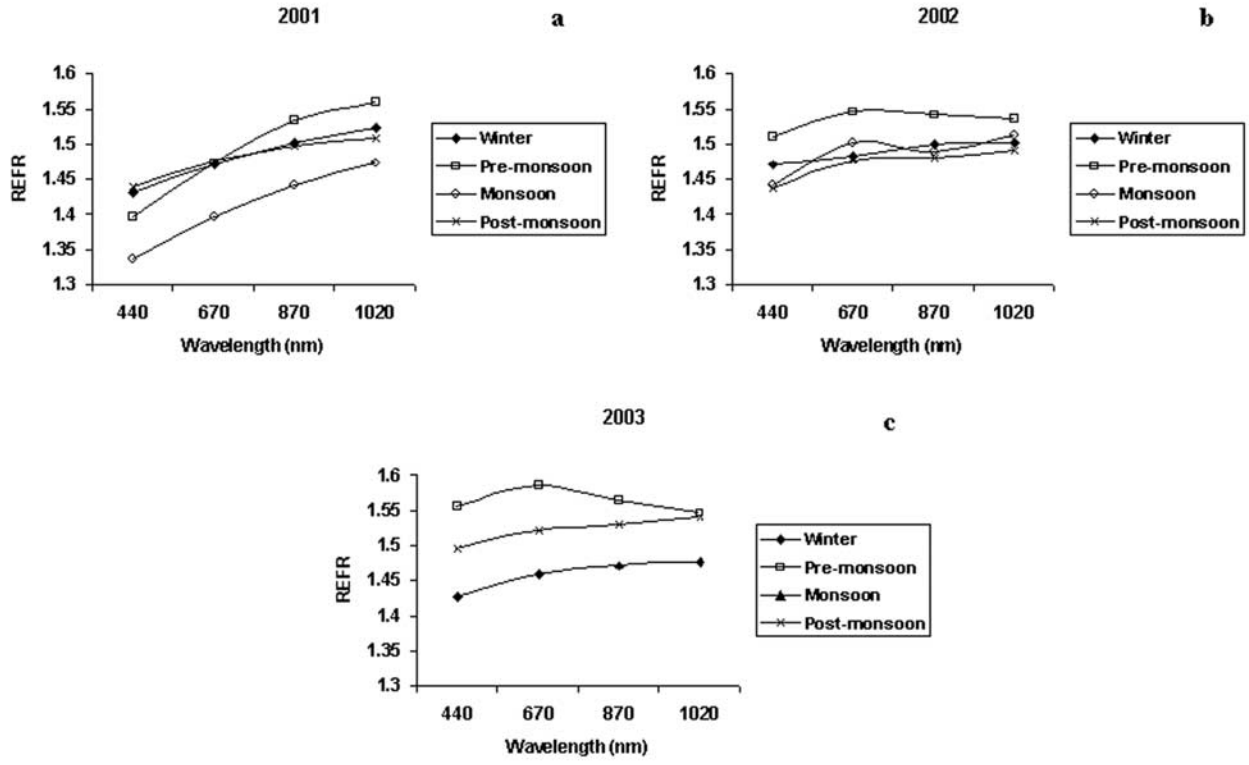

Figure 11. Seasonal variations in $n(\lambda)$ for (a) 2001, (b) 2002, and (c) 2003.

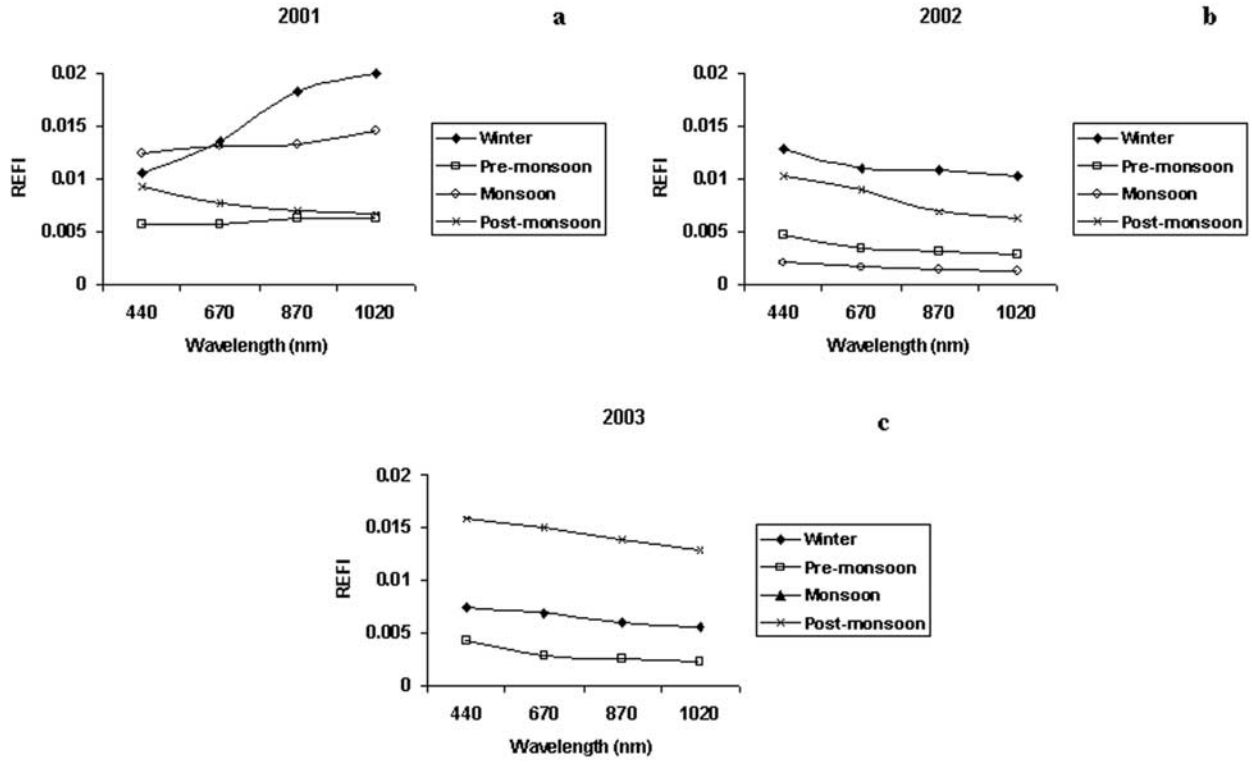

Figure 12. Seasonal variations in $k(\lambda)$ for (a) 2001, (b) 2002, and (c) 2003.

been observed to be different from the years 2001 and 2002 and similar to the variations observed during the winter in the region. This suggests a changing trend in seasonal aerosol loading in the region as also observed from AOD spectra (Figure 2).

3.5. Index of Refraction

[23] The optical properties of the aerosols are described in terms of the index of refraction, obtained by combining real $n(\lambda)$ and imaginary $k(\lambda)$ parts. Imaginary part $k(\lambda)$ quantifies the nature of the absorption, as higher $k(\lambda)$ indicates higher absorption. On the other hand, total scattering increases with increase in $n(\lambda)$ [*Bohren and Huffman*, 1983]. Real and imaginary parts $n(\lambda)$ and $k(\lambda)$ are not independent of SSA and the retrieved size distribution of the aerosols in the region, but some differences in trends may be observed because of the presence of different types of aerosols [*Dubovik et al.*, 2002]. The spectral variations of $n(\lambda)$ and $k(\lambda)$ are shown in Figures 11a–11c and 12a–12c for 2001, 2002, and 2003, respectively. Real part $n(\lambda)$ has been found to increase with λ during all the seasons. The spectral increase in $n(\lambda)$ is maximum during the premonsoon and monsoon seasons, when dust is the dominant component. Real and imaginary parts $n(\lambda)$ and $k(\lambda)$ show contrasting spectral behavior during the years. While $n(\lambda)$ is highest (>1.5) at all wavelengths during the premonsoon season in the years 2002 and 2003, $n(\lambda)$ is found to be highest at larger wavelengths (λ > 670 nm) during the premonsoon season in 2001, showing the higher scattering optical state of the atmosphere during the years 2002 and 2003. This is also supported by the higher SSA in the years 2002 and 2003 compared to that in 2001 (Figure 10). However, lower $n(\lambda)$ values during the monsoon season are probably associated with high relative humidity and resultant hygroscopic growth, similar to the conditions found over Goddard Space Flight Center [*Dubovik et al.*, 2002]. During the premonsoon season, $n(\lambda)$ values at higher wavelengths are close to the $n(\lambda)$ values of dust (1.53) found from several models [*Shettle and Fenn*, 1979; *World Meteorological Organization* (*WMO*), 1983; *Koepke et al.*, 1997], clearly indicating the contribution of dust to the optical properties. However, the $n(\lambda)$ during the postmonsoon and winter seasons have intermediate values.

[24] Imaginary part $k(\lambda)$ has been found to increase with increase in wavelength during the winter season and to decrease during the postmonsoon season in the year 2001, whereas it is almost neutral to the spectral variation during the other seasons. Higher $k(\lambda)$ values (>0.012) indicate the absorbing state of the atmosphere during the winter season in the year 2001; however, the absorbing nature decreases in 2002 and 2003, when $k(\lambda)$ values are found to be low (<0.012) (Figure 12). In fact, $k(\lambda)$ values are found to decrease with an increase in wavelength during the winter season in the last 2 years. Though the spectral behavior of $k(\lambda)$ remains similar during the other seasons in the year 2002, lower $k(\lambda)$ has been observed during the premonsoon and monsoon seasons, which is attributed to the higher dust loading compared to the other years, 2001 and 2003, due to the late monsoon. In fact, the $k(\lambda)$ values in the visible spectrum during this season are similar to the values for dust obtained from several models [*Shettle and Fenn*, 1979; *WMO*, 1983]. During the monsoon season, $k(\lambda)$ values represent aerosols composed of different components, whose variable proportions give rise to the observed interannual variability.

4. Conclusions

[25] This paper presents the seasonal and interannual variability of the aerosol optical properties over an urban-industrial site in the Ganga basin. The main conclusions drawn from our study are summarized as follows:

[26] 1. The aerosol optical properties over Kanpur are found to show a strong seasonal effect with the maximum variability during the monsoon season. The frequency distribution reveals that dust is the major contributor to the optical depth during the premonsoon and monsoon seasons, whereas anthropogenic urban aerosols dominate during the postmonsoon and winter seasons. This region is characterized by different types of aerosol loading by regional air mass, which changes from season to season. The atmospheric processes responsible for the aerosol loading also show strong interannual variation.

[27] 2. Diurnal variations of AOD and α are observed to be maximum during the monsoon season, when aerosols of mixed types are present over the region, whereas WVC shows maximum diurnal variation during the winter season. The diurnal cycle of the local pollutants is clearly observed during the postmonsoon and winter seasons, which is found to be suppressed during the monsoon season.

[28] 3. The aerosol volume size distribution shows bimodal distribution (geometric mean radius is 0.065–0.148 μm for the fine mode and 2.24–3.85 μm for the coarse mode) in general, except during months April–August, when a third mode (modal value of 1–2 μm) appears because of the hygroscopic growth of finer urban aerosols in the presence of abundant atmospheric water vapor. The volume concentrations of aerosol particles of fine and coarse modes are almost similar during the postmonsoon and winter seasons, whereas the coarse mode volume concentration dominates during the time of dust loading.

[29] 4. The SSA observed over Kanpur is found to be highly wavelength dependent (SSA decreases with wavelength) during the winter season because of the dominance of urban (absorbing in nature) aerosols, whereas the reverse trend during the premonsoon and monsoon seasons is attributed to the dominance of the dust (scattering in nature) particles.

[30] 5. Both real and imaginary parts of the refractive index indicate the presence of mixed types of aerosol during the monsoon season. The optical state of the atmosphere is dominantly scattering during the premonsoon and monsoon seasons, whereas during the winter season the nature of the optical state is found to be absorbing. The changing nature of the optical state of the atmosphere seasonally over Kanpur represents loading of the aerosols from different sources, both natural and anthropogenic.

[31] **Acknowledgments.** The CIMEL Sun photometer was deployed on the IIT Kanpur campus under a joint agreement between NASA and IIT Kanpur. The efforts made by Ross Nelson, Alok Sahoo, Sanjeeb Bhoi, and Harish Vishwakarma in running the IIT Kanpur AERONET station are gratefully acknowledged. The authors are grateful to Sanjay Dhande, former Dean of Research and Development and currently Director of IIT

Kanpur, for the deployment and operation of CIMEL at IIT Kanpur. We are also grateful to two anonymous reviewers for their constructive comments.

References

Ackerman, T. P., and O. B. Toon (1981), Absorption of visible radiation in atmosphere containing mixtures of absorbing and non-absorbing particles, *Appl. Opt.*, *20*, 3661–3668.

Ångström, A. (1964), The parameters of atmospheric turbidity, *Tellus*, *16*, 64–75.

Babu, S. S., and K. K. Moorthy (2001), Anthropogenic impact on aerosol black carbon mass concentration at a tropical station: A case study, *Curr. Sci.*, *81*(9), 1208–1214.

Bohren, C. F., and D. R. Huffman (1983), *Absorption and Scattering of Light by Small Particles*, 550 pp., John Willey, Hoboken, N. J.

Cachorro, V. E., R. Vergaz, and A. M. de Frutos (2001), A quantitative comparison of α: A turbidity parameter retrieved in different spectral ranges based on spectroradiometer solar radiation measurements, *Atmos. Environ.*, *35*, 5117–5124.

Charlson, R. J., S. E. Schwartz, J. M. Hales, R. D. Cess, J. A. Coakley Jr., J. E. Hansen, and D. J. Hofmann (1992), Climate forcing by anthropogenic aerosol, *Science*, *255*, 423–430.

Chu, D. A., Y. J. Kaufman, G. Zibordi, J. D. Chern, J. Mao, C. Li, and B. N. Holben (2003), Global monitoring of air pollution over land from the Earth Observing System–Terra Moderate Resolution Imaging Spectroradiometer (MODIS), *J. Geophys. Res.*, *108*(D21), 4661, doi:10.1029/2002JD003179.

Dey, S., S. N. Tripathi, R. P. Singh, and B. N. Holben (2004), Influence of dust storms on the aerosol optical properties over the Indo-Gangetic basin, *J. Geophys. Res.*, *109*, D20211, doi:10.1029/2004JD004924.

Dubovik, O., and M. D. King (2000), A flexible inversion algorithm for retrieval of aerosol optical properties from Sun and sky radiance measurements, *J. Geophys. Res.*, *15*, 20,673–20,696.

Dubovik, O., B. N. Holben, Y. J. Kaufman, M. Yamasoe, A. Smirnov, D. Tanre, and I. Slutsker (1998), Single-scattering albedo of smoke retrieved from the sky radiance and solar transmittance measured from ground, *J. Geophys. Res.*, *103*, 31,903–31,923.

Dubovik, O., A. Smirnov, B. N. Holben, M. D. King, Y. J. Kaufman, T. F. Eck, and I. Slutsker (2000), Accuracy assessments of aerosol optical properties retrieved from Aerosol Robotic Network (AERONET) Sun and sky radiance measurements, *J. Geophys. Res.*, *105*, 9791–9806.

Dubovik, O., B. N. Holben, T. F. Eck, A. Smirnov, Y. J. Kaufman, M. D. King, D. Tanre, and I. Slutsker (2002), Variability of absorption and optical properties of key aerosol types observed in worldwide locations, *J. Atmos. Sci.*, *59*, 590–608.

Eck, T. F., B. N. Holben, J. S. Reid, O. Dubovik, A. Smirnov, N. T. O'Neill, I. Slutsker, and S. Kinne (1999), Wavelength dependence of the optical depth of biomass burning, urban and desert dust aerosol, *J. Geophys. Res.*, *104*, 31,333–31,350.

Eck, T. F., B. N. Holben, O. Dubovik, A. Smirnov, I. Slutsker, J. M. Lobert, and V. Ramanathan (2001), Column-integrated aerosol optical properties over the Maldives during the northeast monsoon for 1998–2000, *J. Geophys. Res.*, *106*, 28,555–28,566.

Eck, T. F., B. N. Holben, J. S. Reid, N. T. O'Neill, J. S. Schafer, O. Dubovik, A. Smirnov, M. A. Yamasoe, and P. Artaxo (2003a), High aerosol optical depth biomass burning events: A comparison of optical properties for different source regions, *Geophys. Res. Lett.*, *30*(20), 2035, doi:10.1029/2003GL017861.

Eck, T. F., et al. (2003b), Variability of biomass burning aerosol optical characteristics in southern Africa during the SAFARI 2000 dry season campaign and a comparison of single scattering albedo estimates from radiometric measurements, *J. Geophys. Res.*, *108*(D13), 8477, doi:10.1029/2002JD002321.

El-Askary, H., R. Gautam, and M. Kafatos (2004), Monitoring of dust storms over Indo-Gangetic Basin, *Indian J. Remote Sens.*, *32*(2), 121–124.

Goloub, P., J. L. Deuze, M. Herman, D. Tanre, I. Chiapello, B. Roger, and R. P. Singh (2001), Aerosol remote sensing over land using the spaceborne polarimeter POLDER, in *Current Problems in Atmospheric Radiation*, edited by W. L. Smith and Yu. M. Timofeyev, pp. 113–116, A. Deepak, Hampton, Va.

Guttikunda, S. K., G. R. Carmichael, G. Calori, C. Eck, and J. H. Woo (2003), The contribution of mega cities to regional sulfur pollution in Asia, *Atmos. Environ.*, *37*(1), 11–22.

Hansen, J., M. Sato, and R. Ruedy (1997), Radiative forcing and climate response, *J. Geophys. Res.*, *102*, 6831–6864.

Holben, B. N., et al. (1998), AERONET: A federated instrument network and data archive for aerosol characterization, *Remote Sens. Environ.*, *66*(1), 1–16.

Hoppel, W. A., J. W. Fitzgerald, and R. E. Larson (1985), Aerosol size distributions in air masses advecting off the east coast of the United States, *J. Geophys. Res.*, *90*, 2365–2379.

Kaufman, Y. J. (1993), Aerosol optical thickness and atmospheric path radiance, *J. Geophys. Res.*, *98*, 2677–2692.

Kim, D.-H., B.-J. Sohn, T. Nakajima, T. Takamura, T. Takemura, B.-C. Choi, and S.-C. Yoon (2004), Aerosol optical properties over east Asia determined from ground-based sky radiation measurements, *J. Geophys. Res.*, *109*, D02209, doi:10.1029/2003JD003387.

Koepke, P., M. Hess, I. Schult, and E. P. Shettle (1997), Global aerosol data set, *Rep. 243*, 44 pp., Max-Planck-Inst. für Meteorol., Hamburg, Germany.

Krishna Moorthy, K., K. Niranjan, B. Narasimhamurthy, V. V. Agashe, and B. V. Krishna Murthy (1999), Aerosol climatology over India: 1. ISRO GBP MWR Network and database, *ISRO-GBP Sci. Rep. 03-99*, Indian Space Res. Organ., Bangalore.

Niranjan, K., Y. R. Babu, G. V. Satyanarayana, and S. Thulasiraman (1997), Aerosol spectral optical depths and typical size distribution at a coastal urban location in India, *Tellus, Ser. B*, *49*, 439–446.

O'Neill, N. T., A. Ignatov, B. N. Holben, and T. F. Eck (2000), The log-normal distribution as a reference for reporting aerosol optical depth statistics: Empirical tests using multi-year, multi-site AERONET sunphotometer data, *Geophys. Res. Lett.*, *27*(20), 3333–3336.

O'Neill, N. T., O. Dubovik, and T. F. Eck (2001), A modified Ångström coefficient for the characterization of sub-micron aerosols, *Appl. Opt.*, *40*(15), 2368–2375.

O'Neill, N. T., T. F. Eck, B. N. Holben, A. Smirnov, A. Royer, and Z. Li (2002), Optical properties of boreal forest fire smoke derived from Sun photometry, *J. Geophys. Res.*, *107*(D11), 4125, doi:10.1029/2001JD000877.

Parameswaran, K. (1998), Atmospheric aerosols and their radiative effects, *PINSA*, *64*, 245–266.

Parameswaran, K., and G. Vijayakumar (1994), Effect of atmospheric relative humidity on aerosol size distribution, *Indian J. Radio Space Phys.*, *23*, 175–188.

Pasricha, P. K., B. S. Gera, S. Shastri, H. K. Maini, A. B. Ghosh, M. K. Tiwari, and S. C. Garg (2003), Role of the water vapor greenhouse effect in the forecasting of fog occurrence, *Boundary Layer Meteorol.*, *107*(2), 469–482.

Ramanathan, V., et al. (2001), Indian Ocean Experiment: An integrated analysis of the climate forcing and effects of the great Indo-Asian haze, *J. Geophys. Res.*, *106*, 28,371–28,398.

Reddy, M. S., and C. Venkataraman (2002), Inventory of aerosol and sulphur dioxide emissions from India: I. Fossil fuel combustion, *Atmos. Environ.*, *36*, 677–697.

Remer, L. A., Y. J. Kaufman, and B. N. Holben (1999), Interannual variation of ambient aerosol characteristics on the east coast of the United States, *J. Geophys. Res.*, *104*, 2223–2231.

Satheesh, S. K., and V. Ramanathan (2000), Large differences in tropical aerosol forcing at the top of the atmosphere and Earth's surface, *Nature*, *405*, 60–63.

Seinfeld, J. H., and S. N. Pandis (1997), *Atmospheric Chemistry and Physics: From Air Pollution to Climate Change*, John Wiley, Hoboken, N. J.

Sharma, M., E. A. McBean, and U. Ghosh (1994), Prediction of atmospheric sulphate deposition at sensitive receptors in northern India, *Atmos. Environ.*, *29*, 2157–2162.

Sharma, M., Y. N. V. M. Kiran, and K. K. Shandilya (2003), Investigations into formation of atmospheric sulfate under high PM_{10} concentration, *Atmos. Environ.*, *37*, 2005–2013.

Shettle, E. P., and R. W. Fenn (1979), Models of aerosols lower troposphere and the effect of humidity variations on their optical properties, *AFCRL Tech. Rep. 79 0214*, 100 pp., Air Force Cambridge Res. Lab., Hanscom Air Force Base, Mass.

Sikka, D. R. (2002), Developments in tropospheric aerosols studies in India, *Indian J. Radio Space Phys.*, *31*, 391–403.

Smirnov, A., N. T. O'Neill, A. Royer, A. Tarussov, and B. McArthur (1996), Aerosol optical depth over Canada and the link with synoptic air mass types, *J. Geophys. Res.*, *101*, 19,299–19,318.

Smirnov, A., B. N. Holben, I. Slutsker, E. J. Welton, and P. J. Formenti (1998), Optical properties of Saharan dust during ACE-2, *J. Geophys. Res.*, *103*, 28,079–28,092.

Smirnov, A., B. N. Holben, O. Dubovik, N. T. O'Neill, L. A. Remer, T. F. Eck, I. Slutsker, and D. Savoie (2000a), Measurements of aerosol optical parameters on US Atlantic coast sites, ships, and Bermuda during TARFOX, *J. Geophys. Res.*, *105*, 9887–9901.

Smirnov, A., B. N. Holben, T. F. Eck, O. Dubovik, and I. Slutsker (2000b), Cloud screening and quality control algorithms for the AERONET data base, *Remote Sens. Environ.*, *73*, 337–349.

Smirnov, A., B. N. Holben, O. Dubovik, N. T. O'Neill, T. F. Eck, D. L. Westphal, A. K. Goroch, C. Pietras, and I. Slutsker (2002a), Atmospheric aerosol optical properties in the Persian Gulf, *J. Atmos. Sci.*, *59*, 620–634.

Smirnov, A., B. N. Holben, Y. J. Kaufman, O. Dubovik, T. F. Eck, I. Slutsker, C. Pietras, and R. N. Halthore (2002b), Optical properties atmospheric aerosol in maritime environments, *J. Atmos. Sci.*, *58*, 501–523.

Smirnov, A., B. N. Holben, T. F. Eck, I. Slutsker, B. Chatenet, and R. T. Pinker (2002c), Diurnal variability of aerosol optical depth observed at AERONET (Aerosol Robotic Network) sites, *Geophys. Res. Lett.*, *29*(23), 2115, doi:10.1029/2002GL016305.

Tegen, I., A. A. Lacis, and I. Fung (1996), The influence on climate forcing of mineral aerosols from disturbed soils, *Nature*, *380*, 419–422.

Venkataraman, C., C. K. Reddy, S. Josson, and M. S. Reddy (2002), Aerosol size and chemical characteristics at Mumbai, India during INDOEX-IFP (1999), *Atmos. Environ.*, *36*, 1979–1991.

World Meteorological Organization (WMO) (1983), Radiation Commission of IAMAP Meeting of Experts on Aerosols and Their Climatic Effects, *Rep. WCP55*, pp. 28–30, Geneva.

S. Dey, V. Tare, and S. N. Tripathi, Department of Civil Engineering, Indian Institute of Technology, Kanpur-208016, India.

B. Holben, Laboratory for Terrestrial Physics, NASA Goddard Space Flight Center, Code 923, Greenbelt, MD 20771, USA.

R. P. Singh, School of Computational Sciences, George Mason University, Fairfax, VA 22030, USA. (rsingh3@gmu.edu)